ChemComm

CrossMark
click for updates

Amorphous vanadium oxide coating on graphene by atomic layer deposition for stable high energy lithium ion anodes†

Xiang Sun,[a] Changgong Zhou,[b] Ming Xie,*[c] Tao Hu,[a] Hongtao Sun,[a] Guoqing Xin,[a] Gongkai Wang,[a] Steven M. George[c] and Jie Lian*[a]

Uniform amorphous vanadium oxide films were coated on graphene *via* atomic layer deposition and the nano-composite displays an exceptional capacity of ~900 mA h g^{-1} at 200 mAg^{-1} with an excellent capacity retention at 1 A g^{-1} after 200 cycles. The capacity contribution (1161 mA h g^{-1}) from vanadium oxide only almost reaches its theoretical value.

Vanadium pentoxide (V_2O_5) is a well-studied material for lithium cathode application due to its high specific capacity, natural abundance, and relatively low cost.[1,2] V_2O_5 possesses multiple redox states similar to other transition metal oxides. If a full reduction of V^{5+} to V^0 is possible, V_2O_5 has a theoretical capacity of 1472 mA h g^{-1}, the highest capacity among all of the metal oxides. Therefore, V_2O_5 can also be an ideal material for high energy anodes. However, limited data are available for V_2O_5 anodes in which the potential high capacity cannot be realized with a stable cycling performance.[3–6] For example, Liu *et al.* reported double-shelled V_2O_5–SnO_2 nano-capsules which exhibit a reversible capacity of 600 mA h g^{-1} at 250 mA g^{-1} after 50 cycles.[3] Poizot reported crystalline V_2O_5 with an initial discharge of 675 mA h g^{-1} which fades completely after 40 cycles.[4] V_2O_5 nanorods displayed 450 mA h g^{-1} at 30 mA g^{-1} after only 20 cycles.[5] A recent study on vanadium oxide aerogels shows a high capacity of 1000 mA h g^{-1} at a rate of 118 mA g^{-1} for only 30 cycles.[6]

The storage of lithium ions in V_2O_5 starts with a reversible intercalation–deintercalation reaction at a potential usually above 1.5 V (*vs.* Li/Li$^+$). It is well known that intercalation below 2 V may cause the structure instability[7] and vanadium dissolution.[8] Further lowering the potential below 1.5 V will introduce decomposition and conversion reactions.[6] The dramatic volume change during charge–discharge will also cause severe pulverization and particle agglomeration. The structural instability and vanadium dissolution eventually lead to significant capacity failure of V_2O_5 as anodes. Vanadium dissolution is also a major drawback for cathode application.

In this study, we deposited vanadium oxide on graphene nanosheets by atom layer deposition (ALD). The vanadium oxide-based graphene composite anode shows a reversible capacity close to 900 mA h g^{-1} at 200 mA g^{-1} and is stable for at least 200 cycles at a greater current density of 1 Ag^{-1}, suggesting no significant capacity loss due to vanadium dissolution. The capacity contribution from V_2O_5 only almost approaches its theoretical limit. We have previously demonstrated that ALD is a viable tool to form metal oxides on carbonaceous substrates for electrochemical applications.[9,10] The strong chemical linkage between carbonaceous substrates and active materials ensures the long cycling stability. In addition, ultrathin films or nano-sized particles formed by ALD will greatly alleviate volume changes compared to their bulk counterparts. Nano-size can further shorten the electron transport and lithium diffusion paths, leading to an enhanced power density. This result further highlights the significance of using ALD to synthesize high energy density electrode materials.

The V_2O_5 ALD was carried out in a static rotary reactor as reported previously.[10] V_2O_5 ALD used vanadyl oxytriisopropoxide with H_2O at 150 °C with a growth rate of ~1 Å per cycle.[1] The higher growth rate in a rotary reactor than in a typical ALD process is due to the insufficient purge of H_2O on high surface area powders, resulting in additional CVD growth.[11] After ALD deposition, the density of the V_2O_5–G nano-composite is much higher than that of the pristine graphene powder (Fig. S1, ESI†). A better volumetric energy density is expected for the V_2O_5–G nanocomposites due to the enhanced density. Thermogravimetric analysis (TGA) indicates that V_2O_5–G contains 59.2 wt% V_2O_5 with as few as 50 cycle V_2O_5 ALD (Fig. S2, ESI†). This is

[a] *Department of Mechanical, Aerospace & Nuclear Engineering, Rensselaer Polytechnic Institute, 110 8th Street, Troy, NY 12180, USA. E-mail: lianj@rpi.edu; Fax: +1-518-276-6025; Tel: +1-518-276-6081*

[b] *Natural Science Department, Lawrence Technological University, Southfield, MI 48075, USA*

[c] *Department of Chemistry and Biochemistry and Department of Chemical and Biological Engineering, University of Colorado at Boulder, Boulder, Colorado 80309, USA. E-mail: Ming.Xie@colorado.edu*

† Electronic supplementary information (ESI) available: Detailed experimental section, optical pictures, TGA data, discharge capacity of graphene, detailed calculation of V_2O_5 contribution, and the SEM image of V_2O_5–G after cycling. See DOI: 10.1039/c4cc04580g
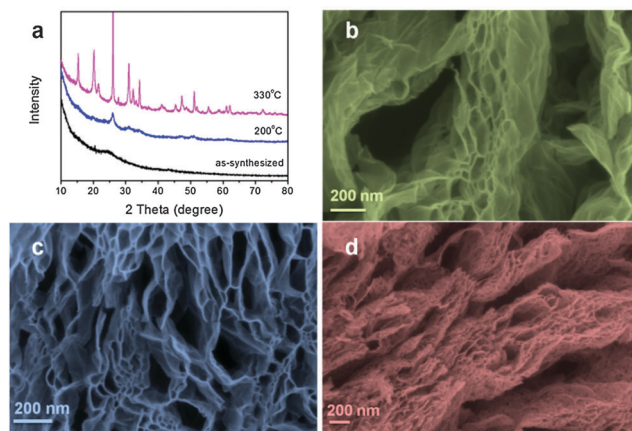
Fig. 1 (a) XRD patterns of as-synthesized and annealed V_2O_5–G; and SEM images of (b) V_2O_5–G, (c) V_2O_5–G annealed at 200 °C, (d) V_2O_5–G annealed at 330 °C.

Fig. 2 (a) Cyclic voltammetry of V_2O_5–G at a scan rate of 0.5 mV s^{-1}; (b) voltage profile of V_2O_5–G at a current density of 200 mA g^{-1}; (c) charge and discharge capacity of V_2O_5–G and annealed V_2O_5–G versus cycle number at a current density of 200 mA g^{-1}; (d) rate performance of V_2O_5–G.

because the rotary reactor allows conformal coating along the 3-D structure of the graphene matrix and high precursor utilization compared to viscous flow-type ALD, which usually requires hundreds of cycles to achieve similar active material mass loadings.[1] From the derivative weight change, the weight loss occurred at 80, 300, and 430 °C, which correspond to the loss of physisorbed water, hydrated water, and burning of graphene, respectively. In order to study the effect of crystallinity and morphology on electrochemical performance, we annealed V_2O_5–G in air at different temperatures. As observed from X-ray diffraction (XRD) patterns in Fig. 1(a), the un-annealed 50 ALD cycle V_2O_5–G shows only a broad graphene diffraction feature with 2θ at 24 degree.[10] No diffraction peaks from crystalline V_2O_5 are observed, indicating the amorphous nature of the as-deposited V_2O_5. After annealing at 200 °C for 1 h, extra broadened diffraction peaks can be observed. Upon further increasing the annealing temperature to 330 °C, the XRD pattern shows intense peaks which can be assigned to the orthorhombic V_2O_5 (JCPDS No. 01-0539).

The pristine graphene shows a wrinkled honeycomb microstructure consisting of thin layered nano-platelets (Fig. S3, ESI†). No agglomerated particles can be seen after deposition, indicating that the V_2O_5 thin film is conformably coated on the surface of graphene. This is a unique advantage of ALD over wet chemistry-based synthesis by which particle agglomeration is usually observed. Post-annealing at 200 °C does not lead to obvious morphological changes (Fig. 1c).

The electrochemical properties of the V_2O_5–G anodes were first examined by cyclic voltammetry at a sweep rate of 0.5 mV s^{-1} and a voltage range from 0.01 to 3 V. As shown in Fig. 2a, in the first discharge cycle, four reduction peaks at 2.78, 2.48, 2.1, and 1.54 V can be related to the multi-step lithium intercalation of V_2O_5, corresponding to the formation of different $Li_xV_2O_5$ phases.[3] In the subsequent charge cycles, two broad peaks at 1.9 and 2.7 V can be assigned to the de-intercalation of the $Li_xV_2O_5$ phases, and each peak might contain a multi-electron transfer process. In the subsequent cycles, surprisingly, the redox peaks located at above 1.5 V eventually diminished; while another
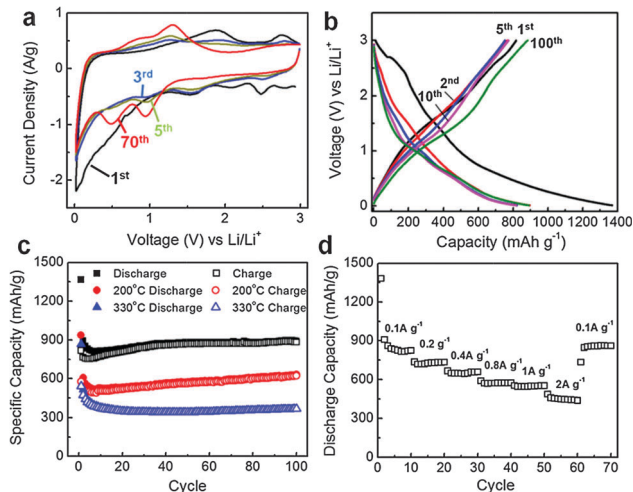
two pairs of redox peaks at 0.49/0.82 V and 0.93/1.3 V started to emerge. These peaks were eventually stabilized and became the major contributors to the charge storage. A similar behaviour can be observed from the voltage profile (Fig. 2b), where the voltage plateaus at above 1.5 V gradually disappeared. It is well known that the lithium storage occurs through intercalation above 1.5 V while decomposition and conversion reactions dominate at below 1.5 V. A recent X-ray photoelectron spectroscopy (XPS) study[6] has revealed that the capacity storage in vanadium oxide aerogel anodes involves decomposition followed by conversion. Therefore, we conclude that the V_2O_5 in our study first undergoes the decomposition reaction forming the VO_x phase, and then follows the conversion reaction to V_2O and Li_2O. These two reactions were found to be highly reversible. The formation of V_2O at the end of the discharge cycle is due to the improbability of the V^{1+} to V^0, which was also confirmed by the recent XPS study.[6] Thus, the practical theoretical capacity of V_2O_5 is 1178 mA h g^{-1}, corresponding to an 8-electron redox reaction.

The significant irreversible capacity loss during the first charge–discharge cycle can be attributed to the formation of SEI. It is also interesting to note that the discharge capacity remains almost constant or becomes greater after the first cycle, although the capacity contribution eventually changes. The vanadium involved in the intercalation reactions at the beginning may gradually evolve into the decomposition and conversion reactions, and the capacity stabilizes after ~10 cycles. The long-term cycle stability of the amorphous and annealed V_2O_5–G is compared in Fig. 2c. The as-synthesized V_2O_5–G showed slightly decreased capacity in the first five cycles and then the capacity kept increasing for the rest of the cycles. This increase in capacity is possibly due to the improved wetting of the high surface area materials[12] and the proton exchange mechanism.[1] The reversible capacity was 892 mA h g^{-1} after 100 cycles, compared to 893 mA h g^{-1} for the 2nd cycle, indicating close to 100% capacity retention. After subtracting the capacity contribution
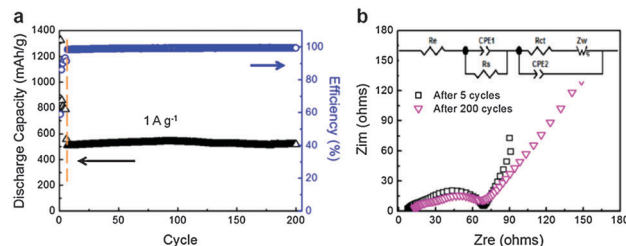
Fig. 3 (a) Discharge capacity and coulombic efficiency for V_2O_5–G at 1 A g^{-1} for 200 cycles; (b) Nyquist plots of V_2O_5–G after 5 and 200 charge–discharge cycles at 1 A g^{-1}. Inset: equivalent circuit model for impedance analysis, where Re is the electrolyte resistance, and Rs and CPE1 are the resistance and capacitance of the surface film formed on the electrodes, respectively. Rct and CPE2 are the charge-transfer resistance and double-layer capacitance, respectively. Zw is the Warburg impedance related to the diffusion of lithium ions into the electrodes.

from graphene only (Fig. S4, ESI†), we can calculate the actual V_2O_5 contribution (see the ESI† for calculations) to be 1161 mA h g^{-1}, very close to the theoretical capacity ($\sim$1178 mA h g^{-1}).

The excellent cyclic stability (*e.g.*, 200 mA g^{-1} to 100 cycles (Fig. 2c) and no capacity fading at greater current density to 200 cycles (Fig. 3a)) suggests that typical degradation induced by vanadium dissolution does not occur. The SEI layer formed at low voltage during the first cycle may be stable, preventing further vanadium dissolution.

For V_2O_5–G annealed at 200 °C, the capacity still reached 633 mA h g^{-1} at 100 cycles, although significantly lower than that of the un-annealed one. Interestingly, the capacity increase along cycling was still observed. Upon further increasing the annealing temperature to 330 °C, the V_2O_5–G anode only shows a capacity of 370 mA h g^{-1} and no capacity increase. Together with the TGA analysis, one can conclude that the continuous increase in capacity might be attributed to the hydrated water,[1] existing in the as-synthesized and 200 °C annealed samples, but not in the 330 °C annealed sample. Obviously, amorphous V_2O_5–G is better for lithium storage than crystallized V_2O_5–G, and the capacity decreases upon increasing the crystallization degree. It is surprising to note that all three samples exhibited excellent cycle stability. It was generally observed that vanadium dissolution[13] occurred at voltages below 1.5 V *vs.* Li/Li$^+$, and therefore capacity decay is expected, as V_2O_5 nanorods[5] lost 26% capacity after 20 cycles and double-shelled V_2O_5 nanocapsules can only maintain 70% of their initial capacity after 50 cycles.[3]

The excellent stability of our materials can be attributed to several factors: (1) the strong chemical linkage of V_2O_5 and graphene defined by ALD; (2) the lithium oxide matrix formed by the conversion reaction could act as a protecting layer for vanadium dissolution; (3) the solid-electrolyte interphase (SEI) formed at low potential can also act as a vanadium diffusion barrier;[6] and (4) with the use of graphene as the matrix, the V_2O_5–G could accommodate a substantial volume change and therefore prevent pulverization of active materials. Such interesting findings provide us an innovative solution for preventing vanadium dissolution, which is also a main problem in employing V_2O_5 for lithium cathode application.[1] In order to prevent V_2O_5

dissolution, the voltage can be lowered intentionally during the first cycle (*e.g.*, down to 0.01 V as in this study) to promote the formation of a SEI on the surface of V_2O_5. In fact, we cycled V_2O_5 from 3 to 0.01 V which includes the voltage window for cathode application (3–1.5 V), and a similar benefit may be expected for V_2O_5 cathodes.

The as-synthesized V_2O_5–G also shows excellent rate capability. As shown in Fig. 2d, the ALD nanocomposite preserves 90%, 79%, and 62% of its capacity at 200 mA g^{-1} when the current densities were increased by 2, 4, and 10 times, respectively. We also studied the long-term stability of V_2O_5–G at fast charge–discharge rates. Fig. 3a shows the cycling behaviour of V_2O_5–G at 1 A g^{-1}. The first five cycles were stabilized at 100 mA g^{-1} to ensure enough activation.[14] After 200 cycles, the capacity retention was $\sim$101.4% and the amorphous V_2O_5–G can still deliver a reversible capacity of 519 mA h g^{-1} and maintain a coulombic efficiency of over 99.5%. We attribute the excellent rate performance to the combinational effects of the amorphous thin film morphology of V_2O_5 and conductive 3-D graphene matrix ensuring fast lithium ion diffusion and electron transfer.

We further examined the excellent performance of V_2O_5–G by electrochemical impedance spectroscopy (EIS) analysis. The Nyquist plots were modelled by an equivalent circuit model. As shown in Fig. 3b, the charge transfer resistance is fairly small after 5 cycles, indicating good electronic conductivity of V_2O_5–G and excellent uniformity at the interface. It remains almost the same after 200 cycles, indicating that the repeated charge–discharge did not cause any electronic contact loss even under a large volume expansion.[15] Such a good electrochemical stability is contributed from the strong chemical bonding between V_2O_5 and graphene, and no particle aggregation was observed after cycling (Fig. S5, ESI†).

In summary, amorphous V_2O_5 was synthesized on porous graphene by ALD and tested as a lithium ion battery anode. The electrochemical results reveal an ultra-stable capacity of 892 mA h g^{-1} with V_2O_5 contribution of 1161 mA h g^{-1} approaching its theoretical value. The ALD V_2O_5–graphene composite anode also displays excellent cyclic stability without any capacity fading. Vanadium dissolution, a major problem limiting V_2O_5 for anode applications, can be greatly alleviated. The synergistic combination of conformal coating by ALD on mechanically robust and highly electrically conductive graphene nanosheets, and the formation of a stable SEI represents an innovative approach in designing advanced vanadium oxide-based electrodes to mitigate mechanical degradation and vanadium dissolution.

Notes and references

1 X. Y. Chen, H. L. Zhu, Y. C. Chen, Y. Y. Shang, A. Y. Cao, L. B. Hu and G. W. Rubloff, *ACS Nano*, 2012, **6**, 7948.
2 Y. Wang and G. Z. Cao, *Adv. Mater.*, 2008, **20**, 2251.
3 J. Liu, H. Xia, D. F. Xue and L. Lu, *J. Am. Chem. Soc.*, 2009, **131**, 12086.

4 P. Poizot, S. Laruelle, S. Grugeon, L. Dupont and J. M. Tarascon, *Ionics*, 2000, **6**, 321.

5 A. M. Glushenkov, M. F. Hassan, V. I. Stukachev, Z. P. Guo, H. K. Liu, G. G. Kuvshinov and Y. Chen, *J. Solid State Electrochem.*, 2010, **14**, 1841.

6 V. Augustyn and B. Dunn, *Electrochim. Acta*, 2013, **88**, 530.

7 C. Delmas, H. Cognacauradou, J. M. Cocciantelli, M. Menetrier and J. P. Doumerc, *Solid State Ionics*, 1994, **69**, 257.

8 Y. Wang and G. Z. Cao, *Chem. Mater.*, 2006, **18**, 2787.

9 C. M. Ban, M. Xie, X. Sun, J. J. Travis, G. K. Wang, H. T. Sun, A. Dillon, J. Lian and S. M. George, *Nanotechnology*, 2013, **42**, 424002.

10 X. Sun, M. Xie, G. K. Wang, H. T. Sun, A. S. Cavanagh, J. J. Travis, S. M. George and J. Lian, *J. Electrochem. Soc.*, 2012, **159**, A364.

11 J. A. McCormick, B. L. Cloutier, A. W. Weimer and S. M. George, *J. Vac. Sci. Technol., A*, 2007, **25**, 67.

12 Q. Zhu, N. Chen, F. Tao and Q. M. Pan, *J. Mater. Chem.*, 2012, **22**, 15894.

13 G. Sudant, E. Baudrin, B. Dunn and J. M. Tarascon, *J. Electrochem. Soc.*, 2004, **151**, A666.

14 S. Chaudhari and M. Srinivasan, *J. Mater. Chem.*, 2012, **22**, 23049.

15 P. J. Zuo, G. P. Yin and Y. L. Ma, *Electrochim. Acta*, 2007, **52**, 4878.